
Article:
Miskevich, E., Alshammari, F.K., Yang, W.G. et al. (5 more authors) (2018) Artificial multiferroic structures using soft magnetostrictive bilayers on Pb(Mg1/3Nb2/3)-PbTiO3. Journal of Physics D: Applied Physics, 51. 085001. ISSN 0022-3727

https://doi.org/10.1088/1361-6463/aaa7d7

Artificial multiferroic structures using soft magnetostrictive bilayers on $Pb(Mg_{1/3}Nb_{2/3})$-$PbTiO_3$

E. Miskevich[1], F. K. Alshammari[1], W-G. Yang[1,2], J. Sharp[1], S. Baco[1], Z Leong[1], Q. A. Abbas[1,3] and N. A. Morley[1]

[1] Department of Materials Science and Engineering, University of Sheffield, Sheffield, S1 3JD, UK

[2] School of Engineering, University of California Santa Cruz, Santa Cruz, CA, 95064 USA

[3] Department of Physics, College of Education for Pure Science, University of Anbar, Anbar, Iraq

Corresponding e-mail: n.a.morley@sheffield.ac.uk

Abstract: Artificial multiferroic structures are of great interest as they combine two or more functionalities together. One example of these structures are magnetostrictive films grown on top of piezoelectric substrates; allowing the magnetisation hysteresis loop of the magnetostrictive film to be manipulated using an electric field across the structure rather than a magnetic field. In this paper, we have studied the multiferroic structure NiFe/FeCo/Ti/$Pb(Mg_{1/3}Nb_{2/3})$-$PbTiO_3$ (PMN-PT) as a function of the electric and magnetic field. Soft magnetostrictive bilayer films (NiFe/FeCo) are studied, as often applications require soft magnetic properties (small coercive and anisotropy fields) combined with larger magnetostrictive constants. Unfortunately, FeCo films can have coercive fields that are too large, while NiFe films' magnetostriction constants are almost zero; thus, combining the two together should produce the "ideal" soft magnetostrictive film. It was found that the addition of a thin NiFe film onto the FeCo film reduced the coercive field and remnant magnetisation on the application of an applied voltage in comparison to just the FeCo film. It was also determined that for the NiFe/FeCo bilayer the magnetisation switchability was ~100% on the application of 8kV/cm, which was higher than the monolayer FeCo films at the same applied field, demonstrating improvement of the multiferroic behaviour by the soft magnetic/magnetostrictive bilayer.

1. Introduction

Artificial multiferroic heterostructures have drawn great attention in the last few years, for the ability to manipulate the magnetic properties of magnetic thin films using an electric field rather than a magnetic field [1-7]. The concept is based on the multiferroic idea where more than one ferroic property (magnetic, electric, elastic) are linked such that each property can be manipulated by a different ferroic field i.e. using magnetic or electric or stress fields. This means that a sample's magnetisation can be altered by using either an electric or stress field, or charge polarisation can be changed by using a magnetic field. This opens up a wide range of possibilities and therefore applications, which include magnetoelectric random access memory [8, 9] and magnetoelectric sensors [10, 11].

Although in nature there are few homogenous materials which display multiferroic behaviour, artificial multiferroics which combine two or more materials together to achieve the same outcome are more common. One of these artificial multiferroics are heterostructures consisting of a piezoelectric substrate such as $Pb(Mg_{1/3}Nb_{2/3})$-$PbTiO_3$ (PMN-PT) or $BaTiO_3$ with a thin magnetic film grown on top. The structures are designed so that strain mediated magnetoelectric (ME) coupling occurs. The magnetic film is usually a magnetostrictive material, as these materials have the largest magnetic response on the application of a strain. The basic concept is that an electric field is applied across the piezoelectric which

causes a strain at the surface, thus the magnetic film on the piezoelectric substrate is then strained, which changes the magnetic behaviour, normally by changing the magnetisation hysteresis by inducing an easy or a hard axis. This has been shown by many groups, for example Zhang et al. [1] studied the magnetostrictive material Fe-Ga on PMN-PT and found a strong converse magnetoelectric coupling of up to 4.55×10^{-7} sm^{-1}. They also observed a change in the remnant magnetisation of 34% and an increase in the coercive field of 30%. The switchablility (defined as the difference in the normalised remnant magnetisation between 0kV/cm and the max applied electric field) of the structures was limited by the large coercive field (~ 6.4kA/m). Other investigators, Yang et al. [6] studied how the magnetic anisotropy and damping constant of FeCo films changed when grown on PMN-PT and manipulated by the voltage controlled substrate strain. They found that the magnetic anisotropy was enhanced, while the damping constant was decreased. Our previous work [12, 13] investigated how the ME coupling between FeCo films and PMN-PT changed with the introduction of thin magnetic and non-magnetic layers between the film and the substrate. It was found that when thin Metglas (FeSiB) layers were used, that two different magnetisation hysteresis states were achieved at zero applied electric field, depending on whether a large positive or negative electric field was applied [13]. For ultra-thin Ti sandwich layers, these layers change the texture within the FeCo films, which increased the switchability of the magnetisation of the FeCo film from ~70% for no Ti layer to ~95% for 8nm Ti layer [12], thus showing that the morphology of the magnetostrictive layer is important in these structures.

Phuoc et al. [5] studied FeCo/NiFe bilayers on different orientations of PMN-PT to see how substrate orientation influences the electrical tuning of the magnetisation. The NiFe in this case was used as an underlayer of thickness 5nm for a 100nm FeCo film. They found that poling the substrate made a difference to the magnetic hysteresis loop measured and whether anisotropy was observed. Before poling, for all substrate crystal directions, the magnetic films were isotropic, while after poling anisotropy was observed in the films. The dynamic permeability also strongly depended on the crystal direction and the applied voltage. Other methods to investigate the magnetoelectric coupling include anisotropic magnetoresistance (AMR), which was used by Gao et al. [2] to study 10nm NiFe films on PMN-PT, using the voltage across the structure to control the AMR. They determined that the applied voltage via the induced strains reduced the free energy barrier in the NiFe films, which changed the AMR response.

One disadvantage of using FeCo as the magnetostrictive layer is its large coercive field (>10kA/m), which means that 100% switching is not achievable. NiFe is a known soft magnetic material, with a very small coercive field (<2kA/m), but also a very small magnetostriction constant (<2ppm), thus its response to the strain applied by a piezoelectric substrate will be smaller than that of FeCo. In an attempt to achieve a large change in magnetisation from the magnetoelectric coupling between the magnetostrictive film and the piezoelectric substrate, but with a smaller coercive field, magnetostrictive bilayers of NiFe/FeCo are investigated in this work. The FeCo is grown on the piezoelectric substrate so should still have the large ME coupling and thus response to the applied strain, while the NiFe is grown on top of the FeCo to investigate whether the magnitude of the coercive field can be reduced in response to the applied strain, to hence achieve a large switching in magnetisation.

2. Experimental Procedure

To study whether a thin NiFe layer improved the magnetic response of a magnetostrictive/piezoelectric heterostructure, the dependence of the magnetic properties on the NiFe thickness were first studied with the NiFe/FeCo bilayers grown on silicon. Once these films had been characterised, the magnetostrictive bilayers were grown on PMN-PT substrates (Fig. 1). The PMN-PT substrates were bought from CTG Advanced Materials, with crystal orientation (011) and d_{31} =-1200 ~ -1800, with Au electrodes on either side. The bottom Au electrode was left on the substrate, while the top electrode was polished off to

leave a smooth PMN-PT surface for the magnetic films to be grown on. A thin 10nm Ti layer was evaporated onto the PMN-PT substrate, as this had been shown from previous work to give a random texture orientation within the FeCo film, which increases the magnetostriction constant [12]. Before growth the silicon substrates were cleaned using acetone followed by isopropanol alcohol (IPA).

For the magnetostrictive bilayer for both film sets, a 50nm $Fe_{50}Co_{50}$ (FeCo) film was grown at power of 75 W and chamber pressure 5mTorr. The $Ni_{81}Fe_{19}$ (NiFe) film was grown on top at power of 75W and chamber pressure of 4.8mTorr for a range of thicknesses (10 to 50nm). These growth parameters were chosen as they gave good control of the films' thickness and uniformity, with the Ar pressure being the lowest to give a stable plasma, which is important for NiFe film growth [14].

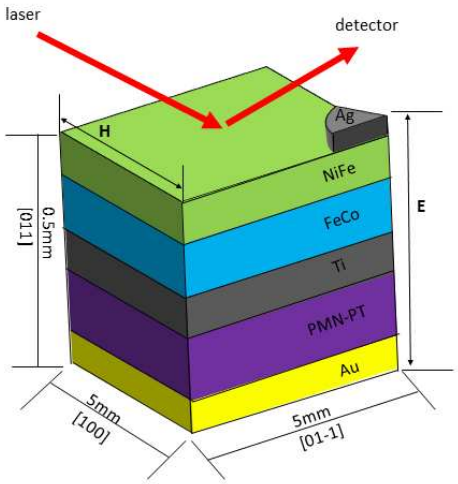

Figure 1. Schematic drawing (not to scale) of the experimental set-up. The electric field is applied across the structure, with the magnetic field applied in the plane of the magnetic films.

The magnetisation hysteresis loops were measured on a magneto-optic Kerr effect (MOKE) magnetometer. First for both film sets, the magnetisation loops were measured with no applied electric field, but as a function of angle between the magnetic field and the sample edge to determine the anisotropy, coercive and anisotropy fields. The magnetostriction of the NiFe/FeCo bilayers was measured using an established technique based on the Villari Effect [14]. Due to the nature of the measurement, only the bilayers grown on the silicon were measured. For the electric field measurements, a specially designed high voltage holder was used, which fitted within the MOKE magnetometer, to allow for the magnetisation hysteresis loops to be measured as a function of applied electric field. A schematic of the set-up is given in Figure 1. The electric field was applied across the whole magnetic/piezoelectric structure for both positive and negative voltages.

The structure of the magnetic/piezoelectric samples were determined using both Transmission electron microscopy (TEM) and x-ray diffraction (XRD). A cross-section transmission electron microscopy (TEM) sample was prepared using the focused ion beam (FIB) lift-out method from the coating surface. The nanolayers' magnetic field was too strong for TEM elemental mapping to be carried out, but the layers were identified by nanobeam electron dispersive spectroscopy (EDS) and bright field images taken in parallel beam TEM mode. The XRD was measured on a PANanlytical X'Pert^3 Powder instrument, the scanning parameter used were step size=0.02; time per step=5.00 s and the scan

speed=0.004^0/s. The wavelength of $K\alpha_1$, λ= 1.540598 Å, the voltage and the current of X-ray source were 45 kV and 40mV, respectively.

3. Results and Discussion

The first set of films were NiFe/50nm FeCo grown on silicon to determine how the thickness of the NiFe changed the bilayer magnetisation response, and whether the two films behaved like one single magnetic film via exchange coupling or two separate films. This behaviour is determined from the magnetocrystalline exchange length of the different layers [15]. The magnetocrystalline exchange length of NiFe and FeCo can be calculated from $L_{ex} \sim \sqrt{A/K_1}$, where A is the exchange stiffness and K_1 is the anisotropy constant. For NiFe, the values A = 13pJ/m and K_1 = 0.5kJ/m are taken to give L_{ex} ~ 161nm and for FeCo A= 63pJ/m and K_1 = 17.5 kJ/m to give L_{ex} ~ 60 nm. Thus both exchange lengths are larger than the magnetic layers being investigated, so the bilayers should behave as a single layer. From Fig. 2 for all the bilayer films studied, a single layer behaviour was observed. This means that the magnetic properties will be a combination of the two different layers. MOKE magnetometry measures the top ~20nm of thin magnetic films, due to the laser attenuation within the film. This penetration distance is known as the skin depth and is dependent on the laser frequency ($4.7x10^{14}$ Hz) and the film resistivity, which for thin NiFe films is known to change as a function of thickness [16]. From previous work [14], a double step was observed in hysteresis loops for similar soft magnetic bilayer films with 25nm top layer thickness, due to the two magnetic layers not being exchanged coupled. As no double step is observed in the Fig. 2, for similar top layer thicknesses, exchange coupling can be assumed, although for the thicker films (>30nm), it is likely that only the top NiFe layer is being measured.

From Fig. 2 it is also observed that as the thickness of NiFe increases the more it dominates the magnetic properties of the bilayer film. The 50nm FeCo film is isotropic (Fig. 2a), while the 25nm NiFe/50nm FeCo has weak uniaxial anisotropy (Fig. 2b) and the 50nm NiFe/50nm FeCo film has strong uniaxial anisotropy (Fig. 2c). The normalised remnant magnetisation was measured as a function of angle (Fig. 2d) and fitted with the following equation [6]:

$$\frac{M_R}{M_S} = D|\cos(\theta - \theta_o)| + C \quad (1)$$

Where D is related to the strength of the uniaxial anisotropy, C is the minimum measured $\frac{M_R}{M_S}$, θ is the angle between the easy axis and the field and θ_o is the angle between the easy axis and the side of the film. For the 50nm NiFe/50nm FeCo film D ~ 1, as it has strong uniaxial anisotropy, while for the 25nm NiFe/50nm FeCo film D ~ 0.16, as it has weak uniaxial anisotropy. For the 50nm FeCo film, as it is isotropic $\theta = \theta_o$ and D = 0 so no variation in M_R/M_s is observed. As there is a change in the anisotropy with NiFe thickness, there is also a change in the anisotropy and coercive fields (Fig. 2e and f). It is observed that both fields decrease as the NiFe thickness increases.

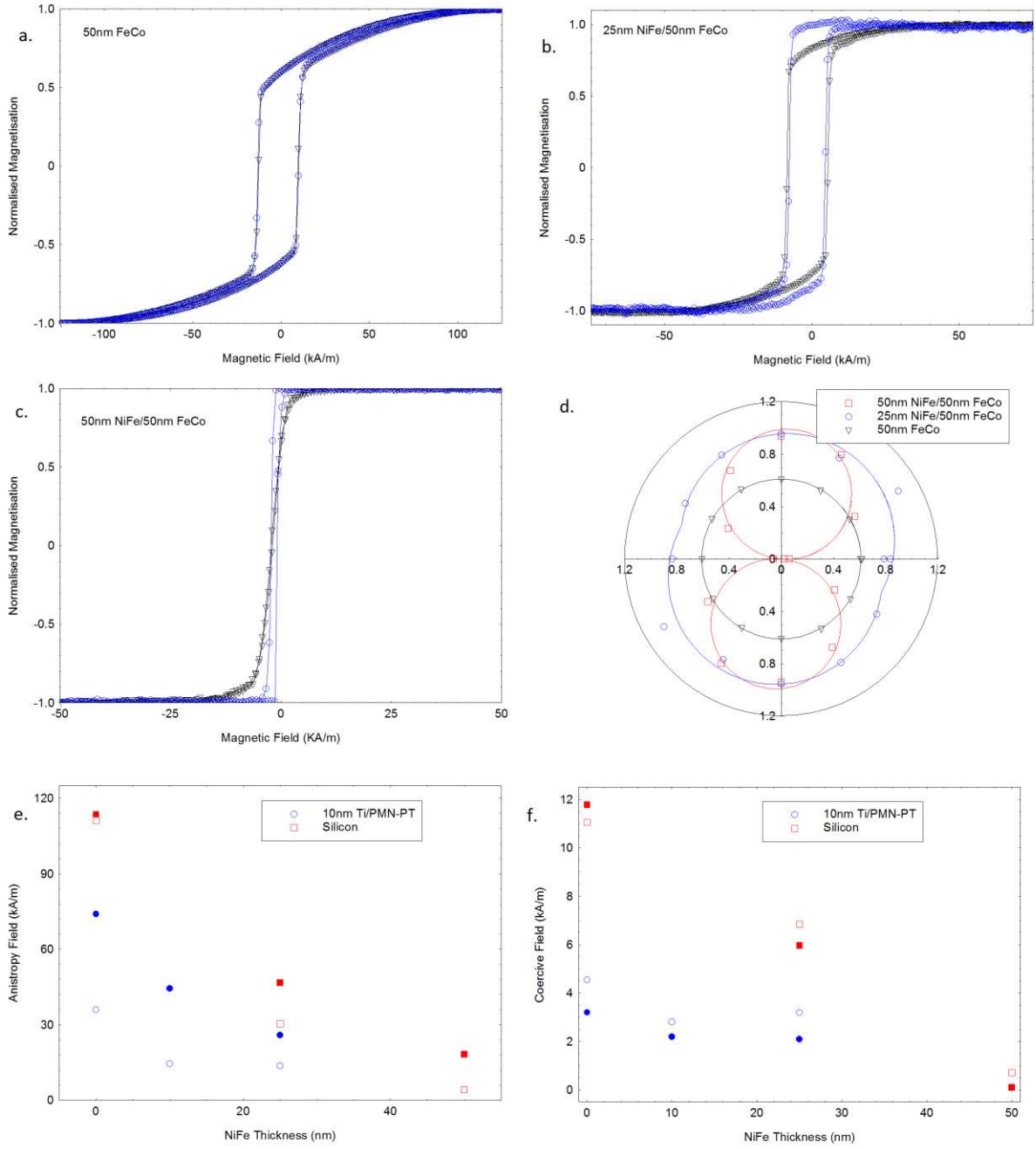

Figure 2.The easy (blue circles) and hard (black triangles) axis magnetisation hysteresis loops of NiFe/50nm FeCo bilayers on silicon, for (a) 0nm NiFe, (b) 25nm NiFe and (c) 50nm NiFe. (d) The remnant magnetisation as a function of magnetic field angle for the different thickness NiFe layers on 50nm FeCo on silicon. The lines are a fit to the data. (e) Anisotropy fields and (f) coercive fields as a function of NiFe thickness on 50nm FeCo on different substrates. The solid shapes are the hard axis and the open shapes for the easy axis.

This is expected, as NiFe is a soft magnetic film, so has smaller anisotropy and coercive fields compared to FeCo. Thus as the NiFe thickness increases, so will the interactions with the FeCo layer. Additionally, the change in anisotropy may also be correlated to the physical structures of both NiFe and FeCo which are known to adopt the FCC structure and the BCC structure, respectively. Since these FeCo films on Si possesses <110> texture perpendicular to the plane (Figure 3a), and the similarity between the kinetic

coefficient (which is related to the interfacial and kinetic properties of the surface) of the (110) BCC Fe and the (100) FCC Fe [17]) suggests that the NiFe surface will possess a (100) texture. From Figure 3, it is observed that the 50nm FeCo film does only have <110> texture, while the 50nm NiFe film has both <111> and <200> texture. For the 50nm FeCo/50nm NiFe film, as the FeCo <110> peak ($2\theta = 44.84^{o}$) and the NiFe <111> peak ($2\theta = 44.27^{o}$) coincide at $2\theta \sim 44^{o}$, this is the larger peak. The NiFe <200> is still observed at $2\theta \sim 51^{o}$. The XRD peaks were fitted using fityk [18], and it was found that for the 50nm NiFe film the ratio of <111> to <200> is 5.5:1, while for the 50nm NiFe/50nm FeCo film, the ratio of NiFe <111> to <200> is 3.4:1. Thus there is an increase in <200> texture in the NiFe film, due to the preference of the NiFe <100> kinetic coefficient at the interface. Thus the easy and hard axis directions for the FCC structure (<111> vs. <100> respectively) are antitheses of those of the BCC structure (<100> vs. <111> respectively). This means that the NiFe magnetisation is "pulling" the FeCo magnetisation around, so that the switching occurs at a lower field. From Figure 4a, the structure of the 10nm NiFe/50nm FeCo/10nm Ti/PMN-PT sample is observed. The deposited layers were found with spot EDS spectra (Fig. 4b) to confirm their compositions for identification. The TEM image is a negative of a bright field image, so vacuum (right of image) appears dark. Layer 1 is the Ti buffer layer, layer 2 is the FeCo film and appears to be made of crystals ~25 nm in width, layer 3 is the NiFe film, layer 4 (pale in TEM image) is the onset of Pt deposition into the top of the NiFe layer, and the top layer is protective Pt deposited during FIB sample preparation. These results are in agreement with the deposition of the thin film layers.

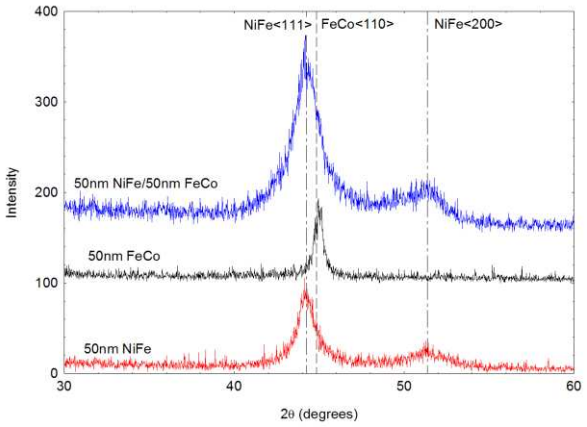

Figure 3a. XRD of 50nm FeCo, 50nm NiFe and 50nm NiFe/50nm FeCo films.

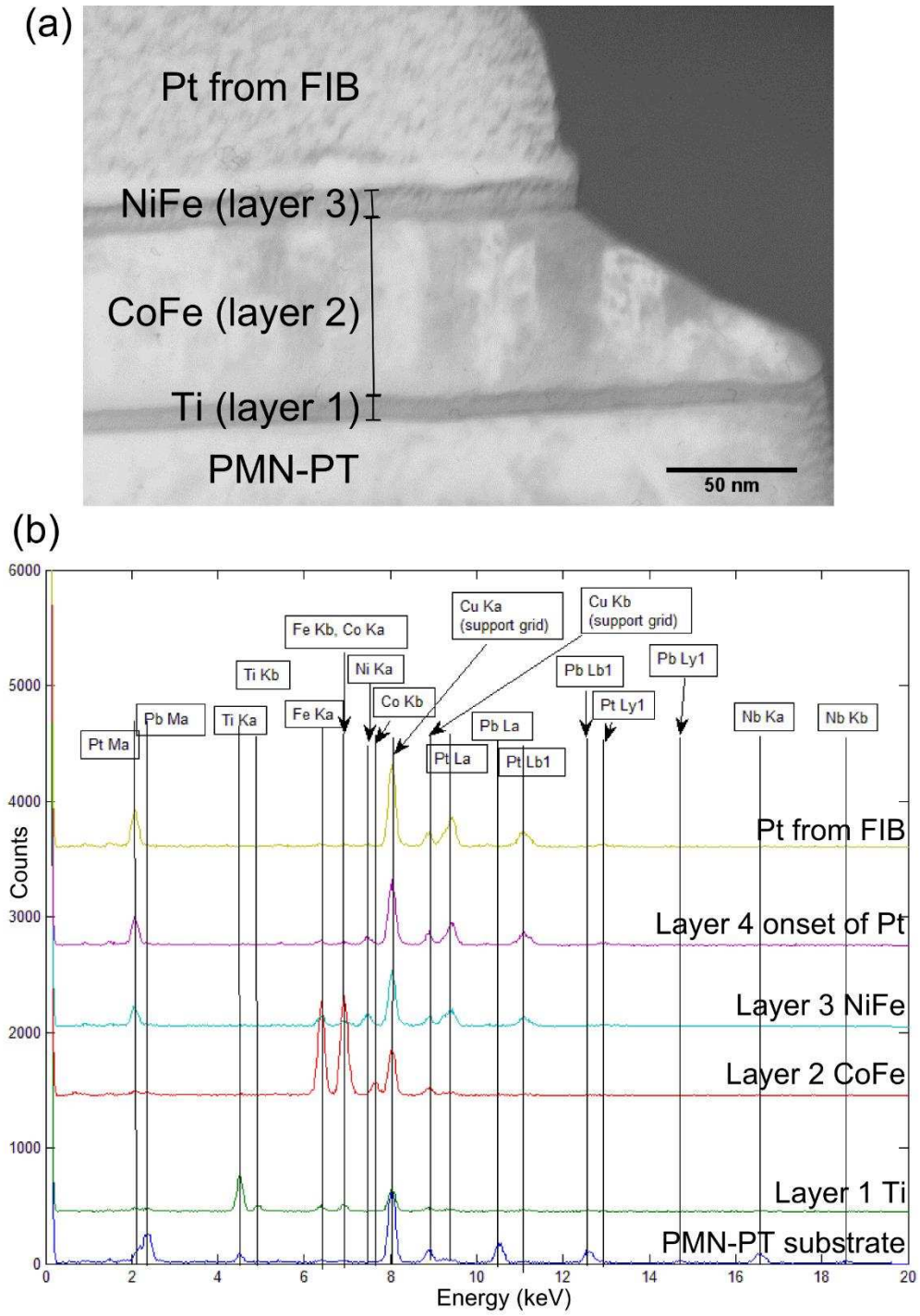

Figure 4a. TEM image of the 10nm NiFe/50nm FeCo/10nm Ti/PMN-PT structure. 4b. EDS spectra for each of the layers in Fig. 4a.

The magnetostriction constants were determined from the NiFe/FeCo bilayers grown on silicon, as a function of NiFe thickness. It was found that the magnetostriction constant was dominated by the FeCo layer. For single layer films, the 50nm FeCo magnetostriction constant was 28 ± 4ppm and the 50nm NiFe magnetostriction constant was ~1ppm. For the 50nm NiFe/50nm FeCo bilayer the magnetostriction constant was 55 ± 4ppm, which is the same order of magnitude as bulk FeCo (λ_s = 66ppm) and larger than the monolayer 50nm FeCo film. Previous work has found that the interface between FeCo and silicon plays a role in the magnitude of the FeCo magnetostriction constant [20],

with it strongly depending on the fabrication method and the film thickness [19], reaching bulk value at thicknesses over a 100nm. The Szymczak model, based on the Neel's model of anisotropy in thin films, describes the change in magnetostriction constant as a function of thickness, given by [20]:

$$\lambda_s = \lambda_v + \frac{\lambda_{s/i}}{t} \quad (2)$$

where λ_v is the volume magnetostriction constant (66ppm for FeCo) and $\lambda_{s/I}$ is the surface/interface magnetostriction constant. Previous work on FeCo/NiFe bilayers found that there was a strong surface/interface magnetostriction constant for FeCo/NiFe [20]. Fitting equation (2) to the magnetostriction constants as a function of NiFe thickness, gives λ_v = 64 ppm and $\lambda_{s/I}$ = -440 ppm/m, which is in good agreement with previous data, which measured $\lambda_{s/I}$ = -402 ppm/m [18]. This means that the FeCo-NiFe interface strongly influences the overall magnetostriction of the bilayers. Hence the NiFe top layer helped to reduce the anisotropy and coercive fields, and increase the magnetostriction constant towards the bulk values.

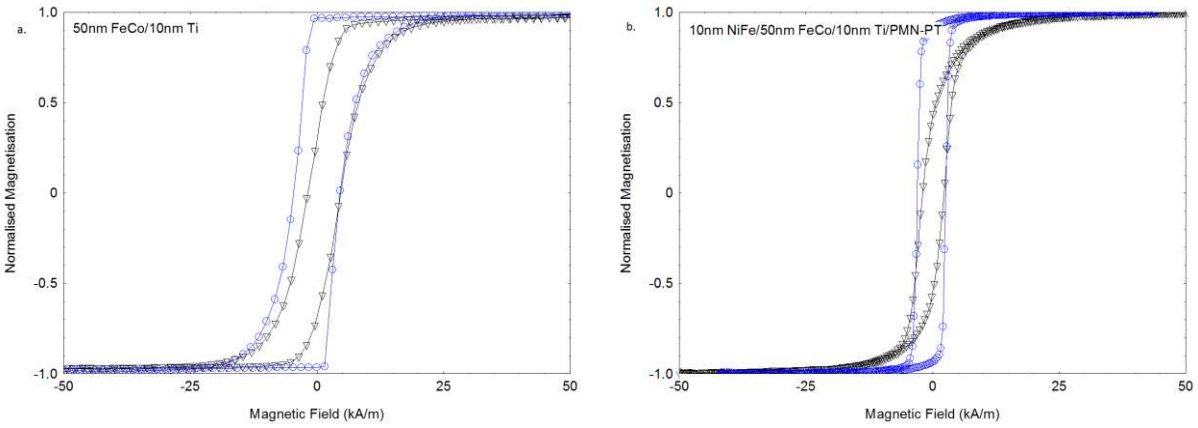

Figure 5. Magnetisation hysteresis loops for (a) 50nm FeCo/10nm Ti/PMN-PT and (b) 10nm NiFe/50nm FeCo/10nm Ti/PMN-PT. The blue circles are the "easy" axis and the black triangles are the "hard axis".

For the bilayers grown on 10nm Ti/PMN-PT, it is observed that again the thin NiFe film changes the overall magnetic behaviour of the films. For the 50nm FeCo structure weak uniaxial anisotropy is observed as different loop shapes are measured as a function of field angle (Fig. 5a). The "hard axis" loop is different from the easy axis loop, but due to the large coercive field the difference in normalised remnant magnetisation is 0.3. From Fig. 2e and f, it is observed that growing FeCo on 10nm Ti reduces the anisotropy field and the coercive field in comparison to the films grown on silicon. This is likely to be due to the Ti helping to promote random grain orientation within the FeCo film [11], as normally FeCo films grown using this deposition system on silicon have a <110> texture perpendicular to the plane (Figure 3). The addition of the 10nm NiFe film increases the uniaxial anisotropy, with the difference between the easy axis and hard axis remnant magnetisation being 0.44 (Fig. 5b). Similar to the NiFe/FeCo films grown on silicon, the anisotropy field and coercive field are both reduced with the addition of the NiFe film on to the FeCo. Although an increase in the NiFe thickness did not decrease the anisotropy and coercive fields further.

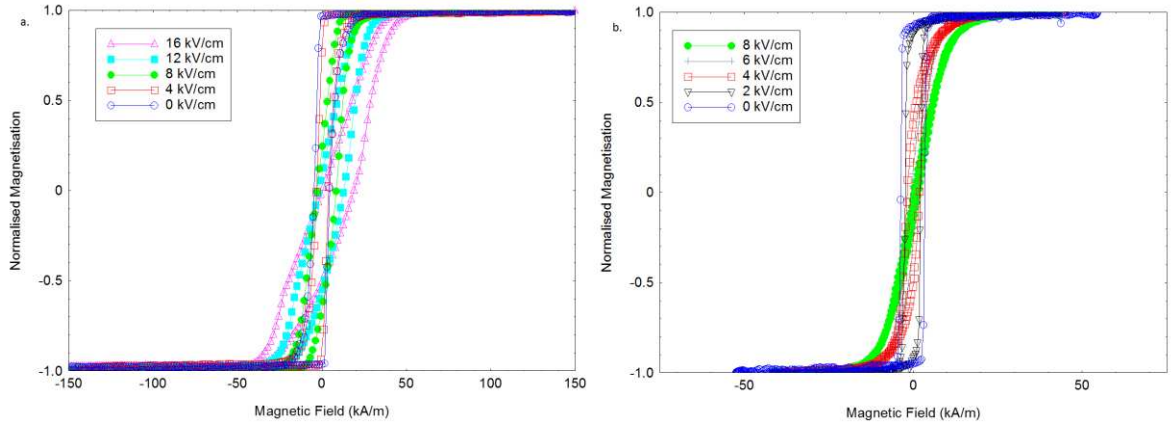

Figure 6. Magnetisation Hysteresis loops for (a) 50nm FeCo/10nm Ti/PMN-PT and (b) 10nm NiFe/50nm FeCo/10nm Ti/PMN-PT as a function of applied electric field

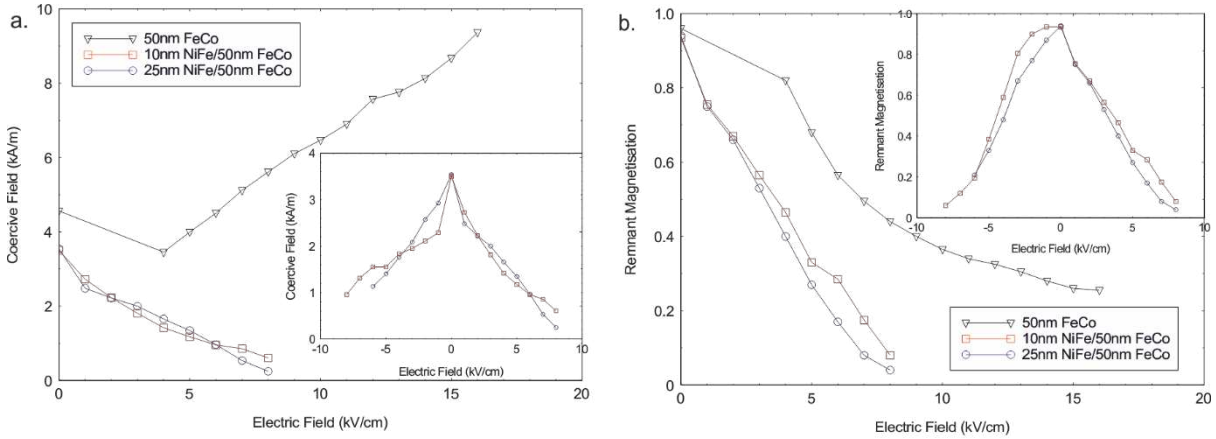

Figure 7. Coercive field (a) and Remnant Magnetisation (b) as a function of applied electric field. The 50nm FeCo/PMN-PT remnant magnetisation as a function of electric field data [12]. Insets for both graphs is the positive and negative electric field dependence for the 10nm and 25nm NiFe/50nm FeCo structure.

The change in the magnetisation hysteresis loops for the 50nm FeCo film and the 10nm and 25nm NiFe/50nm FeCo bilayers grown on 10nm Ti/PMN-PT as a function of the applied electric field across the structure are shown in Fig. 6. For the 50nm FeCo film the hysteresis loop changes from an easy axis loop to a hard axis loop as the electric field increases, with the difference in remnant magnetisation between 0kV/cm and 8kV/cm being ~0.55. The coercive field also strongly changes with electric field, with an initial decrease at 4kV/cm followed by a gradual increase with electric field. This behaviour is not ideal for applications. From the hysteresis loops, it is observed that for the 0kV/cm and 4kV/cm loops, the switching is continuous with a single gradient, while for the loops for higher applied electric fields, there are two different gradients, which suggest that the domain walls within the FeCo film are being pinned possible due to the strain created by the PMN-PT at the interface. This has been observed in thin FeCo films before [7]. For the NiFe/FeCo bilayers, there was very little difference in the loop shape at zero applied field. From Fig. 6 and 7, it is observed as the electric field is increased, again the hysteresis loop changes from an easy axis loop to a hard axis loop, with a difference in the remnant magnetisation between 0kV/cm and 8kV/cm being ~0.95. Thus there is a larger change in the switchability in the hysteresis loops with the addition of the thin NiFe film compared to just the FeCo film. Also the coercive field linearly decreases with increasing electric field, so the issue with domain wall pinning observed in the FeCo film has been overcome by the addition of the NiFe film. As the

NiFe/FeCo bilayers behave as a single magnetic film, this decrease is likely to be due to both the thickness of the film increasing and the NiFe layer reducing the overall coercive field of the structure. The results seem to be independent of the thickness of the NiFe film, as both the 10nm and 25nm NiFe/50nm FeCo coercive fields and remnant magnetisations as a function of positive and negative electric field are similar. The thicker 25nm NiFe film coercive field and remnant magnetisation have a more linear dependence on the applied electric field. This linear dependence with electric field for both positive and negative electric field, is important for MERAM devices, where multi-level non-voltage states are required as a function of electric field [9]. Thus if the magnetic behaviour is linear with electric field, this will make the operation of the devices simpler.

From the remnant magnetisation data the converse magnetoelectric coupling constant, α^E, can be determined. It is calculated from [7]:

$$\alpha = \frac{\mu_o \Delta M_R}{E} \tag{3}$$

Where ΔM_R is the change in remnant magnetisation at an applied electric field, E and zero electric field. The ME coupling constants were calculated for each of the different structures at 8kV/cm, for the 50nm FeCo film $\alpha^E = 1.51 \times 10^{-6} sm^{-1}$, while for the 10nm NiFe/50nm FeCo film $\alpha^E = 2.2x10^{-6} sm^{-1}$ and for the 25nm NiFe/50nm FeCo film $\alpha^E = 2x10^{-6} sm^{-1}$. Thus the ME coupling increased with the addition of the NiFe layer, due to the increase in ΔM_R, dominating the coupling. The calculated values are in good agreement with our previous work, where for a 65nm FeCo/PMN-PT structure $\alpha^E = 2.5x10^{-6} sm^{-1}$ at 9kV/cm [7].

The disadvantage of the FeCo/PMN-PT structure was that the coercive field was 5kA/m at 9kV/cm, which is an order of magnitude larger than the NiFe/FeCo/Ti/PMN-PT structures coercive fields. Thus the addition of the NiFe layer has maintained the high ME coupling constant, while reducing the coercive fields. As the ME coupling of the NiFe/FeCo bilayers on PMN-PT is the same or better than the FeCo films, this means that the high magnetostriction constant measured for the NiFe/FeCo films on silicon is maintained when grown on PMN-PT.

The magneto-electric coupling co-efficient, α, is defined as either direct or converse [21], depending on whether a magnetic field or an electric field is applied to the device. In this paper, the measurements were taken using the remanence magnetisation technique [20], which provides a single value of the electrically induced ME co-efficient α^E also known as the converse ME co-efficient. Other methods used to determine the magneto-electric coupling include magnetically induced measurement, piezoelectric measurement and using scanning probe microscopy [22]. For the magnetically induced ME measurements, the induced voltage across the structure is measured as a function of an applied ac magnetic field and a dc bias magnetic field, to give the ME voltage coupling, α_V^H, which is related to α^H by the relative permittivity $\varepsilon_o\varepsilon_r$, and is also known as the direct ME co-efficient [21]. For the magnetically induced measurements, the ME voltage coupling strongly depends on the frequency of the ac magnetic field and the dc bias field magnitude, thus non-linear values are obtained for α_V^H. For example, for multilayers of 10-40 µm $CoZnFe_2O_4$-PZT, the ME voltage coupling at 500 Oe is ~250mV/cm.Oe, while at 2000 Oe, α_V^H ~50 mV/cm.Oe [23]. This method is generally used for thick magnetostrictive/piezoelectric bilayers and laminates. Some of the highest α_V^H measured for magnetostrictive/piezoelectric bilayer and laminates include α_V^H = 22 V/cm.Oe for 25 µm FeSiBC/100 µm PZT [24] and α_V^H = 4.9 V/cm.Oe for Terfenol-D/PZT/Terfenol-D trilayers [25].

The method used in this paper hides the complex non-linear behaviour of the ME voltage coupling. To compare the different ME coupling values, the α^E determined in this paper is converted into V/cm.Oe, which is the measured units of α_V^H. Thus for the 10nm NiFe/50nm FeCo structure, $\alpha^E = 2.2x10^{-6} sm^{-1}$, which gives α_V^H ~ 126 V/cm.Oe. This is an order of magnitude higher than those measured using the magnetic induced measurement [24, 25]. The reasons for this difference, could be due to the

magnetostrictive films in our structures being at least an order of magnitude thinner than the other examples magnetostrictive layers, plus our magnetostrictive films are grown directed onto the piezoelectric substrates, while for the other structures the magnetostrictive layers are epoxied onto the piezoelectric layer. Thus the ME coupling in these structures will also depend on the epoxy, including its thickness, which is likely to reduce the coupling.

4. Conclusions

By combining a soft magnetic layer (NiFe) with a magnetostrictive layer (FeCo), an artificial multiferroic structure with a large ME coupling and small coercive field was produced. The addition of the thin NiFe layer to the FeCo/Ti/PMN-PT structure changed the anisotropy of the magnetic bilayers, while maintaining the high magnetostriction constant, thus improving the response of the magnetic layers to the applied electric field. This improvement in the switchability of the magnetic films at lower electric fields means that the overall working power will be lower compared to just the FeCo/Ti/PMN-PT structure. This is important for devices such as MERAM, which aim to have multi-level non-volatile states achieved at low power to be commercially attractive [9].

Acknowledgements

EM and NAM would like to acknowledge the SURE scheme for providing funding for the project.

References

[1] Y. Zhang, Z. Wang, Y. Wang, C. Lou, J. Li and D. Viehland, "Electric field induced strain modulation of magnetisation in Fe-Ga/Pb($Mg_{1/3}Nb_{2/3}$)-$PbTiO_3$ magnetoelectric heterostructures", Journal of Applied Physics, 115, 084101, (2014)

[2] Y. Gao, J. Hi, L. She and C. W. Nan, "Strain mediated voltage control of magnetism in multiferroic $Ni_{77}Fe_{23}$/Pb($Mg_{1/3}Nb_{2/3}$)$_{0.7}Ti_{0.3}O_3$ heterostructures", Applied Physics Letters, 104, 142908 (2014)

[3] T. Jin, L. Hao, J. Cao, M. Liu, H. Dang, Y. Wang, D. Wu, J. Bait and F. Wei, "Electric field control of anisotropy and magnetisation switching in CoFe and CoNi thin films for magnetoelectric memory devices", Applied Physics Express, 7, 043002, (2014)

[4] T. Nan, Z. Zhou, M. Liu, X. Yang, Y. Gao, B. A. Assaf, H. Lin, S. Velu, X. Wang, H. Lou, J. Chen, S. Akhtar, E. Hu, R. Rajiv, K. Krishna, S. Sreedhar, D. Herman, B. M. Howe, G. J. Brown and N. X. Sun, "Quantification of strain and charge co-mediated magnetoelectric coupling on ultra-thin Permalloy/PMN-PT interface" Scientific Reports, 4, 3688, (2014)

[5]N. N. Phuoc and C. K. One "Role of crystal orientation on electrical tuning of dynamic permeability in strain-mediated multiferroic structures", Materials Research Express, 4, 066101, (2017)

[6] C. Yang, F. Wang, C. Zhang, C. Zhou and C. Jiang "Tuning magnetic anisotropy and the damping constant using substrate induced strain in a FeCo/Pb($Mg_{1/3}Nb_{2/3}$)$_{0.7}Ti_{0.3}O_3$ heterostructure", J. Physics. D: Applied Physics, 48, 435001, (2015)

[7] W-G. Yang, N. A. Morley, J. Sharp and W. M. Rainforth, “Giant electric field tunable magnetic properties in a $Co_{50}Fe_{50}$/lead magnesium niobate-lead titanate multiferroic heterostructure”, Journal of Physics D: Applied Physics, 48, 305005, (2015)

[8] M. Bibes and A. Barthelemy, “Towards a magnetoelectric memory”, Nature Materials, 7, 425-426, (2008)

[9] J. Shen, J. Cong, D. Shang, Y. Chai, S. Shen, K. Zhai and Y. Sun, “A multilevel non-volatile magnetoelectric memory”, Scientific Reports, 6, 34473, (2016)

[10] J. Gutierrez, A. Lasheras, P. Martins, N. Pereira, J. M. Barandiaran and S. Lanceros-Mendez, “Metallic Glass/PVDF magnetoelectric laminates for resonant sensors and actuators: a review”, Sensors 17, 1251, (2017)

[11] C. Israel, N. D. Mathur and J. F. Scott, “A one-cent room temperature magnetoelectric sensor”, Nature Materials, 7, 93-94, (2008)

[12] W-G. Yang, N. A. Morley, J. Sharp, Y. Tian and W. M. Rainforth, “Strain-mediated converse magnetoelectric coupling strength manipulated by a thin titanium layer”, Applied Physics Letters, 108, 012901, (2016)

[13] W-G. Yang, N. A. Morley and W. M. Rainforth, “Electric field-controlled magnetisation in bilayered magnetic films for magnetoelectric memory”, Journal of Applied Physics, 118, 034102, (2015)

[14] A. Caruana Finkel, N. Reeves-McLaren and N. A. Morley, “Influence of soft magnetic underlayers on the magnetic properties of $Co_{90}Fe_{10}$ films”, Journal of Magnetism and Magnetic Materials, 357, 87-92, (2014)

[15] G. S. Abo, Y-K. Hong, J. Park, J. Lee, W. Lee and B-C Choi, “Definition of Magnetic Exchange Length”, IEEE Transactions on Magnetics, 49, 8, 4937 – 4939, (2013)

[16] R. M. Valletta, G. Guthmiller and G. Gorman, “Relation of thickness and some physical properties of NiFe thin films”, Journal of Vacuum Science & Technology A: Vacuum, Surfaces and Films, 9, 2093, (1991)

[17] D. Y. Sun and M. Asta, “Crystal-melt interfacial free energies and mobilities in fcc and bcc Fe”, Physical Review B, 69, 174103, (2004)

[18] M. Wojdyr, “Fityk: a general-purpose peak fitting program”, J. Appl. Cryst. 43, 1126-1126, (2010)

[19] N. A. Morley, S. Rigby and M. R. J. Gibbs, “Anisotropy and magnetostriction constants of nanostructured $Fe_{50}Co_{50}$ films”, Journal of Optoelectronics and Advanced Materials, 1, 2, 109-113, (2009)

[20] S. Kotapati, A. Javed, N. Reeves-McLaren, M. R. J. Gibbs and N. A. Morley, “Effect of the $Ni_{81}Fe_{19}$ thickness on the magnetic properties of $Ni_{81}Fe_{19}/Fe_{50}Co_{50}$ bilayers”, Journal of Magnetism and Magnetic Materials, 331, 67-71, (2013)

[21] M. Staruch, J. F. Li, Y. Wang, D. Viehland, and P. Finkel, “Giant magnetoelectric effect in nonlinear Metglas/PIN-PMN-PT multiferroic heterostructure”, Appl. Phys. Lett. 105, 152902 (2014)

[22] M. M. Vopson, Y. K. Fetisov, G. Caruntu and G. Srinivasan, “Measurement techniques of the magneto-electric coupling in multiferroics”, Materials, 10, 963, (2017)

[23] G. Srinivasan, E. T. Rasmussen, and R. Hayes “Magnetoelectric effects in ferrite-lead zirconate titanate layered composites: The influence of zinc substitution in ferrites” Physical Review B 67, 014418 (2003)

[24] S. Dong, J. Zhai, J. Li, and D. Viehland, “Near-ideal magnetoelectricity in high-permeability magnetostrictive/piezofiber laminates with a (2-1) connectivity”, Appl. Phys. Lett. 89, 252904 (2006)

[25] J. Zhai, Z. Xing, S. Dong, J. Li and D. Viehland, “Magnetoelectric laminate composites: An overview”, Journal of the American Ceramic Society, 91, 2, 351-358, (2008)